MR IMAGING OF WATER AND FAT IN CORTICAL BONE: COMPARISON BETWEEN THE SWIFT AND FSE SEQUENCES

Luning Wang[1] and Qun Zhao[1]
[1]*Department of Physics and Astronomy, University of Georgia, Athens, GA, United States*

Target audience: Scientists and clinicians who are interested in imaging of short T_2 materials such as cortical bones, water and/or fat suppressions.

Purpose: Bone imaging is of critical importance as bone diseases, such as osteoporosis, have influenced millions of people's lives. However, because of its short T_2/T_2* values, cortical bone is usually 'invisible' for MRI when using conventional pulse sequences [1]. In recent years, the ultrashort echo time (UTE) sequence has been successfully applied to image components, such as bound water, in cortical bone [2]. In this work, we performed MR imaging of a swine humerus bone before and after dehydration using both the fast spin echo (FSE) and the sweep imaging with Fourier transformation (SWIFT) sequences [3]. In addition, water and fat saturations were conducted to separate water and fat in the bone.

Methods: A piece of 2 cm-in-length bone segment was cut from a fresh swine humerus bone and immerged into a 2% agar gel to prevent water loss. MR scans were immediately conducted on a 7 T Varian Magnex scanner (Agilent Technologies, Santa Clara, CA) after the agar gel solidified. The 2D FSE sequence (TR/TE = 3 s/10.25 ms, ETL = 8, FOV = 7 cm, thk = 1 mm, size = 512^2, avg = 4) and the 3D SWIFT sequence ($\theta = 8°$, TR = 4 ms. Spokes = 64,000 spokes, FOV = 7 cm, avg =3) were used to generate morphologic images of the humerus bone. In order to discriminate water and fat components, suppression pulses were added for both sequences by using a 4 ms Gaussian pulse with 120°/90° flip angles, followed by a 2 ms gradient crusher, respectively. After MR imaging, the bone segment was removed from the agar gel and the bone marrow was removed. To further remove free water from the bone, dehydration was conducted by first immersing the humerus bone into 99% ethanol for 24 hours, and then air-dried at about 500°C for 20 minutes. The dehydrated bone segment was placed into Fomblin solution to improve field homogeneity for the additional MR scan by using the same protocols listed above. A vial of water (0.3 mL) was attached to the container that held the bone as a reference.

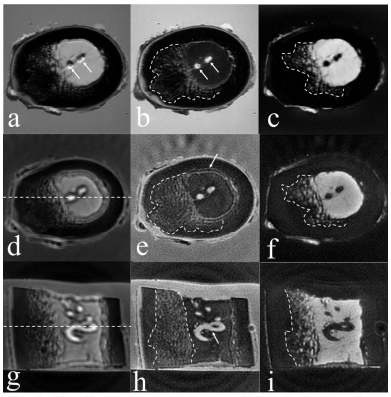

Fig. 1. This figure shows the images of a fresh humerus bone acquired using the FSE (1st row) and SWIFT sequences (2nd and 3rd rows). Fat and water suppressions were applied for the images in the second and third columns, respectively.

Results: Fig. 1 shows MR images of the fresh humerus bone. Fig. 1(a) is a coronal image acquired by using the regular FSE sequence. Because of chemical shift, the canals in the bone marrow were shifted along the frequency encoding (vertical) direction in Fig. 1(a), indicated by the arrows. In Fig. 1(b), fat signal was suppressed by a RF pulse. Because of the relatively long TE, only the free water signal was observed in Fig. 1(b), such as the cross-section of the canals pointed by the arrows with clear boundaries but without chemical shift artifact. With fat saturation, the distribution of free water in the cortical bone, represented as white dots, can now be determined in Figure 1(b) in the area enclosed by the dashed curve, though the signal intensity is weak. Figure 1(c) shows the fat distribution in the humerus bone after water suppression. The canals are now shown as dark holes in the image, and the fat component in the cortical bone is surrounded by the dashed curve. Figs. 1(d) and 1(g) are the coronal and axial images of the humerus bone obtained using the regular SWIFT sequence. Their relative positions are indicated by the horizontal, dashed lines in the two figures. Since the SWIFT sequence utilizes the radial k-space sampling, the artifacts caused by chemical shift appeared as circular-shape blurring artifact compared with Fig. 1(a). Figs. 1(e) and 1(h) illustrate the water distribution in the humerus bone using fat suppression, and clear boundaries of different components can be depicted. For example, in Fig. 1(h), as indicated by the arrow, the canals were clearly delineated. Additionally, compared with Fig. 1(b), more water components can be better viewed inside the cortical bone, enclosed by the dashed curves, benefiting from the ultra-short echo time of the SWIFT sequence. Figs. 1(f) and 1(i) show the fat distribution after water suppression. The outer boundary of fat inside the cortical bone was traced by the dashed curves, and tissues consisting of water, such as the canals, were suppressed and appeared dark.

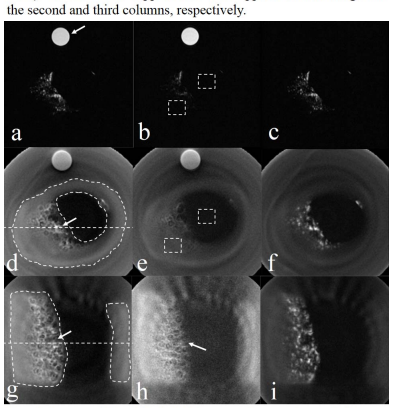

Fig. 2. Images of the dehydrated humerus bone and a vial of water were acquired using the FSE (1st row) and SWIFT sequences (2nd and 3rd rows). Fat and water suppressions were applied for the images in the second and third columns, respectively.

Fig. 2 shows MR images of the dehydrated cortical bone. Figs. 2(a) to 2(c) are the coronal images acquired using the FSE sequence. A vial of water, pointed by the arrow in Fig. 2(a), was shown as a reference. Since the bound water has a T_2 value in the scale of hundreds microsecond, only the fat component and the vial of water were seen in the FSE image. In Fig. 2(b), after fat suppression was applied, little signal from the fat remained in the cortical bone probably due an inhomogeneous B_1 field. The CNR between the two rectangular boxes is nearly zero, indicating the FSE sequence is not suitable to detect bound water in the cortical bone. In Fig. 2(c), after the vial of water was suppressed, the residual fat has a similar distribution as observed in Fig. 2(a). Figs. 2(d) and 2(g) illustrate the SWIFT images of the cortical bone on coronal and axial slices, and their relative positions are indicated by the horizontal, dashed lines in the two figures. The cortical bone became visible and its boundaries were delineated by the dashed curves. Bubble-like blurring caused by chemical shift is pointed by the arrows in the two images. With fat saturation, Figs. 2(e) and 2(h) mainly illustrate the bound water component of the cortical bone. The CNR between the two rectangular boxes in Fig. 2(e) is about 17.4, much higher compared with the FSE images. With water saturation, the signal from water vial was completely suppressed in Fig. 2(f), and fat distribution in the cortical bone was depicted in Figs. 2(f) and 2(i).

Discussion: A swine humerus bone was scanned before and after dehydration using the FSE and SWIFT sequences. Fat and water saturations were conducted to differentiate water and fat components. The free water and fat have a relatively long T_2/T_2* values, so they can be visualized well by use of the FSE sequence. However, the FSE sequence failed to image the bound water in the cortical bone, as demonstrated in Figs. 2(a) and 2(b). On the contrary, by shortening the echo time to a few microseconds, the SWIFT sequence has the advantage of catching signal from short T_2* materials. As demonstrated by the CNR values, the dehydrated cortical bone can be visualized and detected by using the SWIFT sequence. Furthermore, in order to visualize the bound water better, one has to suppress signals from free water and fat, otherwise the signals of the latter are too strong to make bound water visible. In this work, we utilized fat saturation in order to investigate the bound water remained in a dehydrated bone. But such an objective may also be achieved by implementation of RF pulses to suppress free water and fat simultaneously, with a drawback of suffering more loss of SNR.

Conclusion: Fresh and dehydrated swine humerus bone was imaged by using the FSE and SWIFT sequences to visualize water and fat components of the cortical bone. The SWIFT sequence demonstrated its unique advantage over the FSE sequence on acquiring signal from materials of short T_2* values, i.e., bound water in cortical bone in this study.

References: [1] Reichert IL et al, MRI 2005;23(5):611-618. [2] Du J et al, NMR in biomed. 2013;26(5):489-506. [3] Idiyatullin D et al, JMR 2006;181(2):342-349.